AD-A175 788 THE UPPER ATMOSPHERE COMPOSITION SPECTROMETER(U) 1/1
AEROSPACE CORP EL SEGUNDO CA SPACE SCIENCES LAB
D C KAYSER ET AL. 30 SEP 86 TR-0086(6940-04)-1
UNCLASSIFIED SD-TR-86-77 F04701-85-C-0086 F/G 4/1 NL

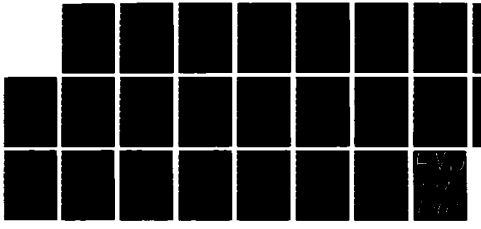

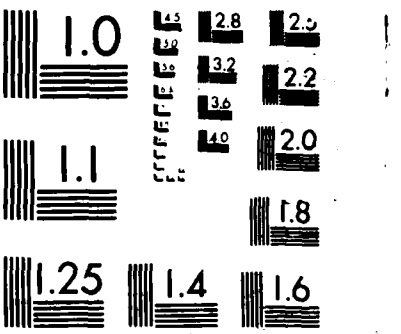
1.0
1.1
1.25
1.4
1.6
1.8
2.0
2.2
2.8
3.2
3.6
4.0

(12)

REPORT SD-TR-86-77

AD-A175 788

The Upper Atmosphere Composition Spectrometer

D. C. KAYSER, W. T. CHATER,
C. K. HOWEY, and J. B. PRANKE
Space Sciences Laboratory
Laboratory Operations
The Aerospace Corporation
El Segundo, CA 90245

30 September 1986

Prepared for

SPACE DIVISION
AIR FORCE SYSTEMS COMMAND
Los Angeles Air Force Station
P.O. Box 92960, Worldway Postal Center
Los Angeles, CA 90009-2960

This report was submitted by The Aerospace Corporation, El Segundo, CA 90245, under Contract No. F04701-85-C-0086 with the Space Division, P.O. Box 92960, Worldway Postal Center, Los Angeles, CA 90009-2960. It was reviewed and approved for The Aerospace Corporation by H.R. Rugge, Director, Space Sciences Laboratory. Maj Edmund Daszewski/WE was the project officer for the Mission Oriented Investigation and Experimentation (MOIE) program.

This report has been reviewed by the Public Affairs Office (PAS) and is releasable to the National Technical Information Service (NTIS). At NTIS, it will be available to the general public, including foreign nationals.

This technical report has been reviewed and is approved for publication. Publication of this report does not constitute Air Force approval of the report's findings or conclusions. It is published only for the exchange and stimulation of ideas.

Edmund D. Daszewski

EDMUND D. DASZEWSKI, Maj, USAF
MOIE Project Officer
SD/WE

Joseph Hess

JOSEPH HESS, GM-15
Director, AFSTC West Coast Office
AFSTC/WCO OL-AB

UNCLASSIFIED

SECURITY CLASSIFICATION OF THIS PAGE *(When Data Entered)*

REPORT DOCUMENTATION PAGE		READ INSTRUCTIONS BEFORE COMPLETING FORM
1. REPORT NUMBER SD-TR-86-77	2. GOVT ACCESSION NO. ADA175788	3. RECIPIENT'S CATALOG NUMBER
4. TITLE *(and Subtitle)* The Upper Atmosphere Composition Spectrometer		5. TYPE OF REPORT & PERIOD COVERED 6. PERFORMING ORG. REPORT NUMBER TR-0086(6940-04)-1
7. AUTHOR(s) David C. Kayser, William T. Chater, Charles K. Howey, and James B. Pranke		8. CONTRACT OR GRANT NUMBER(s) F04701-85-C-0086
9. PERFORMING ORGANIZATION NAME AND ADDRESS The Aerospace Corporation El Segundo, Calif. 90245		10. PROGRAM ELEMENT, PROJECT, TASK AREA & WORK UNIT NUMBERS
11. CONTROLLING OFFICE NAME AND ADDRESS Space Division Los Angeles Air Force Station Los Angeles, Calif. 90009-2960		12. REPORT DATE 30 September 1986 13. NUMBER OF PAGES 29
14 MONITORING AGENCY NAME & ADDRESS*(if different from Controlling Office)*		15. SECURITY CLASS. *(of this report)* Unclassified 15a. DECLASSIFICATION/DOWNGRADING SCHEDULE

16. DISTRIBUTION STATEMENT *(of this Report)*

Approved for public release; distribution is unlimited.

17. DISTRIBUTION STATEMENT *(of the abstract entered in Block 20, if different from Report)*

18. SUPPLEMENTARY NOTES

19. KEY WORDS *(Continue on reverse side if necessary and identify by block number)*

Atmospheric Composition; Neutral-Mass Spectrometers; Satellites; Wind; Temperature

20 ABSTRACT *(Continue on reverse side if necessary and identify by block number)*

The Upper Atmosphere Composition Spectrometer (UACS) was flown on the DOD Space Test Program mission S85-1. This report describes the instrument and its operation. The Upper Atmosphere Composition Spectrometer employs a conventional quadrupole mass filter with a semiopen ionization chamber and a special dual detector system for a large dynamic measurement range. In addition to measuring neutral gas composition for masses 4 to 48, UACS performs a retarding potential analysis of the incident neutral gas stream to measure atmospheric temperature and one component of the neutral wind. Examples of its operation in orbit are discussed.

DD FORM 1473 (FACSIMILE)

UNCLASSIFIED

SECURITY CLASSIFICATION OF THIS PAGE *(When Data Entered)*

PREFACE

The authors would like to thank former and present directors of the Space Sciences Laboratory, G. A. Paulikas and H. R. Rugge, respectively, and J. M. Straus, head, Atmospheric Sciences Department for their continued support of this research. Members of the Aerospace Space Test Directorate-Planning and Operations Department provided invaluable assistance in the areas of mission planning and experiment integration. Expertise in the installation and use of the vacuum-cap cutter mechanism was furnished by D. McIntyre of the University of Minnesota Physics Machine Shops.

CONTENTS

FIGURES

INTRODUCTION

In the last two decades satellite-borne neutral composition experiments have contributed substantially to our understanding of the dynamics and chemistry of the earth's upper atmosphere. Furthermore, in conjunction with charged particle and remote sensing measurements, they have provided the detailed observations needed to improve our understanding of the basic physics of auroral and solar heat inputs, as well as satisfying more immediate needs for improved empirical models of composition. Over time, composition measurement techniques have been modified and improved, giving in recent years greater measurement accuracy and versatility. Presently, with the exception of atomic hydrogen, routine density measurements of all significant thermospheric species can be made at altitudes between 130 and 1000 km. Techniques for the measurement of neutral wind and temperature were developed later, and are still being refined.

In consequence, the present data base for the neutral upper atmosphere is extensive but uneven with regard to measurement accuracy and completeness. Most recently, Hedin[1] discussed the need for additional coverage at high latitudes during high solar activity, as well as coverage at low altitudes generally. Disagreements between in situ- and remotely-sensed temperature data are other areas that warrant further measurements. It is thus desirable that measurements of the neutral thermosphere be continued for the foreseeable future, preferably into the period of next solar maximum (~ 1992).

The Upper Atmosphere Composition Spectrometer (UACS) was designed to operate on low-flying satellites and make measurements of the neutral thermosphere that would augment the existing composition data base. It would also allow the investigation of the usefulness of some largely untried measurement

concepts. UACS is designed to make routine composition measurements of He, O, N_2, Ar, and O_2. Atomic and molecular oxygen separation follows techniques described in Nier et al.[2] and Kayser and Potter.[3] The "fly-through" analysis of Nier et al.[2] has been extended to allow a full retarding potential energy analysis (RPA) of the incident gas stream, thereby affording another technique for measurement of neutral temperature and wind. This RPA technique complements the baffle method of Spencer et al.[4] and Spencer et al.[5] and was described as a feature of the Dynamics Explorer Wind and Temperature Spectrometer.[5] However, to date no results have been published which demonstrate that RPA has been successfully applied to neutral composition measurements. It will be seen that even though UACS employs an electrostatic quadrupole mass filter in the style of the closed-source sensor described by Peltz et al.,[7] its measurement concept resembles the one used in the so-called quasi-open source mass spectrometer of Nier et al.[6]

UACS was recently flown on a DOD Space Test Program mission, S85-1. The mission was flown in a polar, nearly circular orbit at approximately 200 km altitude, thus providing a suitable environment for evaluation of our design. While this report is intended primarily to describe the instrument, we are also able to show preliminary flight data which illustrate its major operational features.

TECHNIQUE

The technique used for satellite-based mass spectrometer measurements of composition relies on two underlying relationships: The first relationship prescribes the ion source number density, N_s, of each gas species as a function of ambient density, N_a. For example, following the derivation of Hedin et al.,[8] when the ion source region consists of a spherical thermalizing

chamber, N_s is given by

$$N_s = N_a\{\sqrt{T_a/T_s}\ F(S)\ \cos^2(\theta/2) + 1\} \qquad (1)$$

where

$$F(S) = \exp(-S^2) + \pi^{1/2}S[1+\mathrm{erf}(S)],$$

and

$$S = [m/(2kT_a)]^{1/2}\ V\cos\phi.$$

Here T_a and T_s are respectively the ambient and source temperature, θ is the half-angle of the chamber orifice as measured from entrance normal, m is the species mass, k is Boltzmann's constant, V is the satellite velocity (plus any wind component in the ram direction) and ϕ is the gas ram angle measured from entrance normal. Consideration of Eqn. 1 for V=8000 m/s and small ram angles shows that N_s is essentially independent of T_a. For UACS the F(S) term of Eqn. 1 requires modification to account for a more complex source geometry.

A second relationship is required to specify the proportionality between the instrument detector output and the ionizing chamber gas density. Because this proportionality depends on numerous design details, the needed relationship must be determined by calibration. Combined, the two relationships allow a determination of ambient density from instantaneous detector output in a manner that is insensitive to ambient wind and temperature. These latter quantities must be determined separately. One method of wind and temperature measurement[4] modulates the incident gas flow

with an external mechanical baffle, and the resulting signal variation is analyzed to yield temperature and cross-wind components. The ram component of the wind must be obtained by yet another method, as detailed below.

Evaluation of Eqn. 1 with typical parameter values shows that gas density in the thermalization chamber is largely determined by the term involving F(S), which represents the contribution of the thermalized out-flowing gas component, while the contribution of the streaming inflowing gas (term 2) is small. For example, at satellite velocities, the ratio of terms is 60:1 or more for N_2. Conventional mass spectrometer operation cannot distingush between these components and thus produces a sum of signals nearly proportional to the larger thermalized gas density. However, when a streaming particle is ionized by electron bombardment it retains the signature of the ambient gas, namely velocity and direction imparted by bulk motion of the gas, V, plus a thermal velocity, v, representative of the ambient thermal distribution function, f(v,m)dv. With a velocity V=8 km/s in the satellite reference frame, the ion will have a typical energy of .33 ev/AMU, compared with .005 ev/AMU or less for an ion derived from the thermalized gas of the ion source. A 2-volt potential barrier at the ion source exit will, as a consequence, pass streaming ions of O, N_2 and O_2 (5.3, 9.2 and 10.6 volts typical) while repelling thermal ions. Composition, temperature and large cross-winds (on spun satellites) have been successfully measured with mass spectrometers modified in this manner.[2,9,10]

Sweeping the potential barrier to achieve a full retarding potential analysis of the streaming gas energy distribution, and hence temperature and wind, is a logical extension of the barrier technique. Figure 1 is a plot of typical particle energy distributions f(E,m) obtained when f(v,m) is transformed into the satellite reference frame. Because the energy analysis is

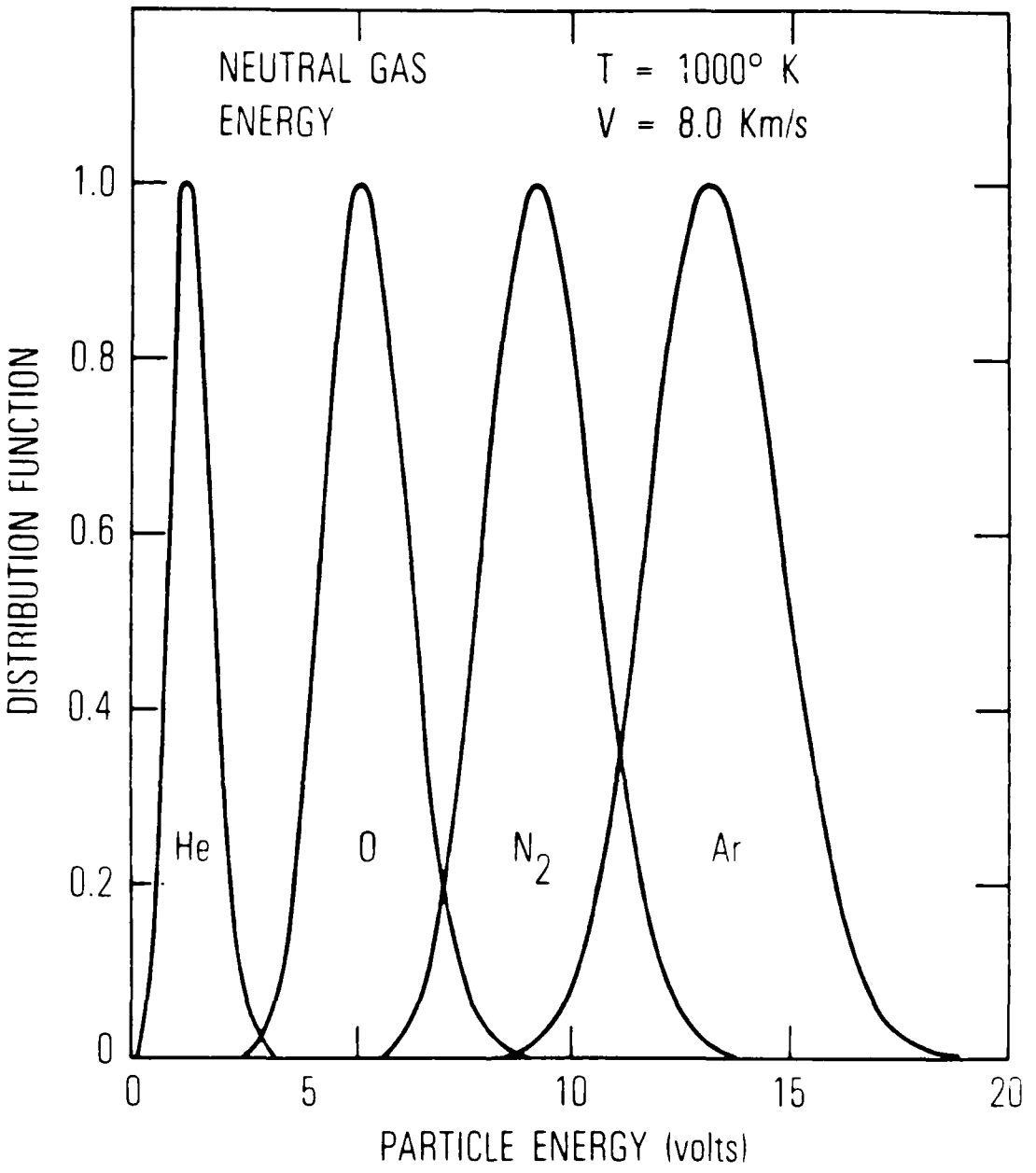

Fig. 1. Neutral Particle Energy Distributions in the Satellite Reference Frame of 8 km/s for Typical Gases He, O, N_2, and Ar. Ambient neutral temperature of 1000 K and no wind component in the ram direction are assumed.

done with a flat grid, f(E,m) describes only the ram component of energy. No information on cross-wind components is obtained from this method. It should be noted that the species distributions overlap extensively, implying that an energy analysis without mass separation would be ambiguous. A wind component, dV, in the ram direction will shift the distributions in energy by the fraction dE/E = 2dV/V. As an example, a 100 m/s wind will shift the N_2^+ distribution maximum from 9.3 to 9.53 volts, an easily detected change. Distribution width is a measure of the ambient gas temperature.

The signal obtained from the RPA analysis is in the form of a cumulative distribution curve, that is, the signal represents the population of all particles with energies greater than the instantaneous barrier voltage. Figure 2 shows three such curves, corresponding to T_a = 1000 K, and winds of +200, 0, and -200 m/s in the ram direction. For simplicity, the calculation assumes no energy discrimination after the RPA grid. The change in curve shape with temperature is illustrated in Figure 3. These distributions correspond to typical extremes (700-1500 K) encountered in daytime measurements above 200 km altitude.

The wind component can be obtained directly from shifts in the position of the RPA curve after accounting for the satellite velocity. Based on the above graphical illustration, accuracies of 50 m/s or better should be obtainable without elaborate processing. Extraction of temperatures accurate to 5% K or better may require refined numerical techniques which account for instrumental transfer characteristics and the resultant curve distortion. In a later section of the present work we include examples of RPA curves obtained by UACS on S85-1. These preliminary data are consistent with design expectations.

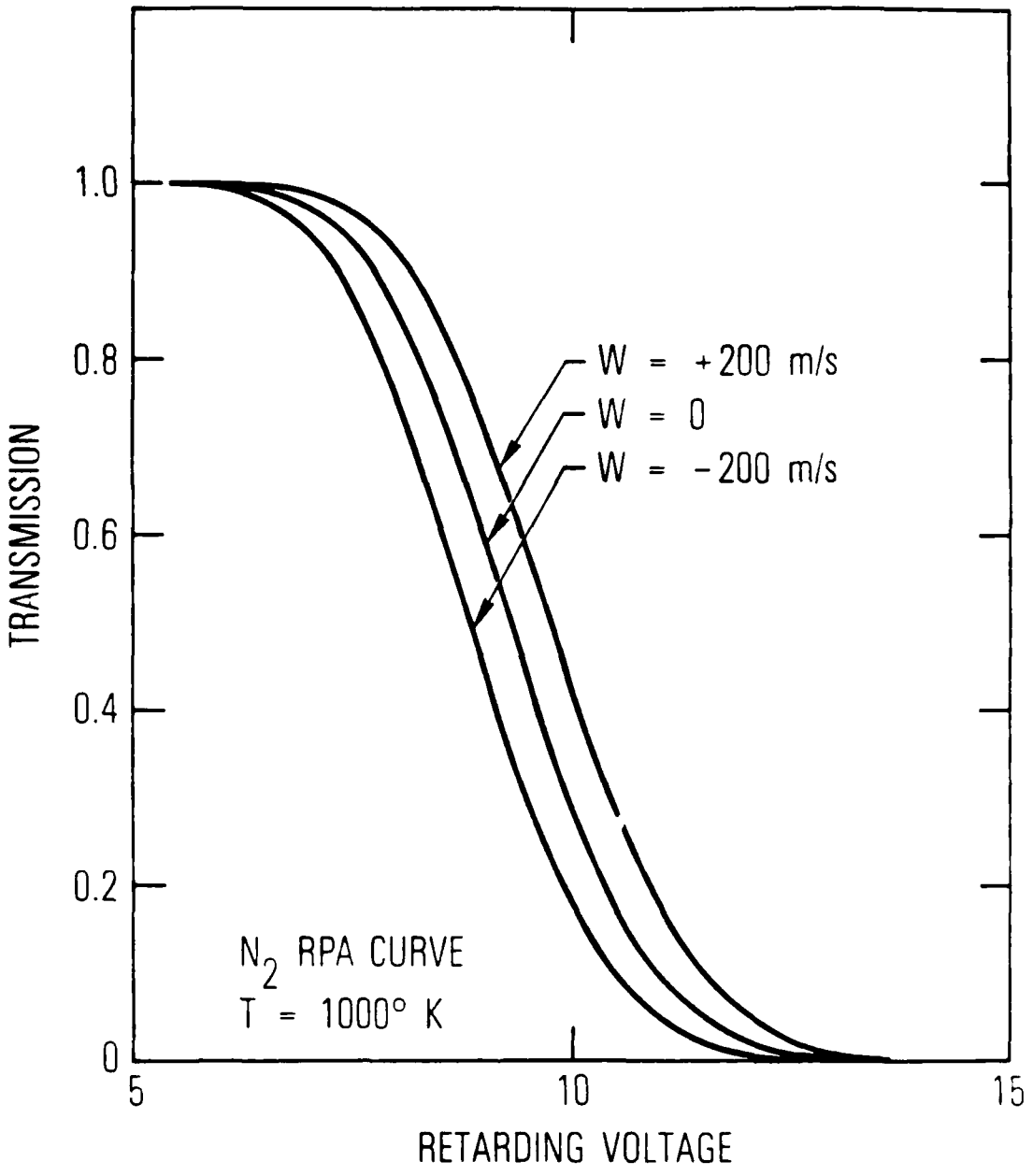

Fig. 2. Idealized Retarding Potential Transmission Curves for N_2 at an Ambient Neutral Temperature of 1000 K. Curves show the displacement effect of ±200 m/s winds in the ram direction.

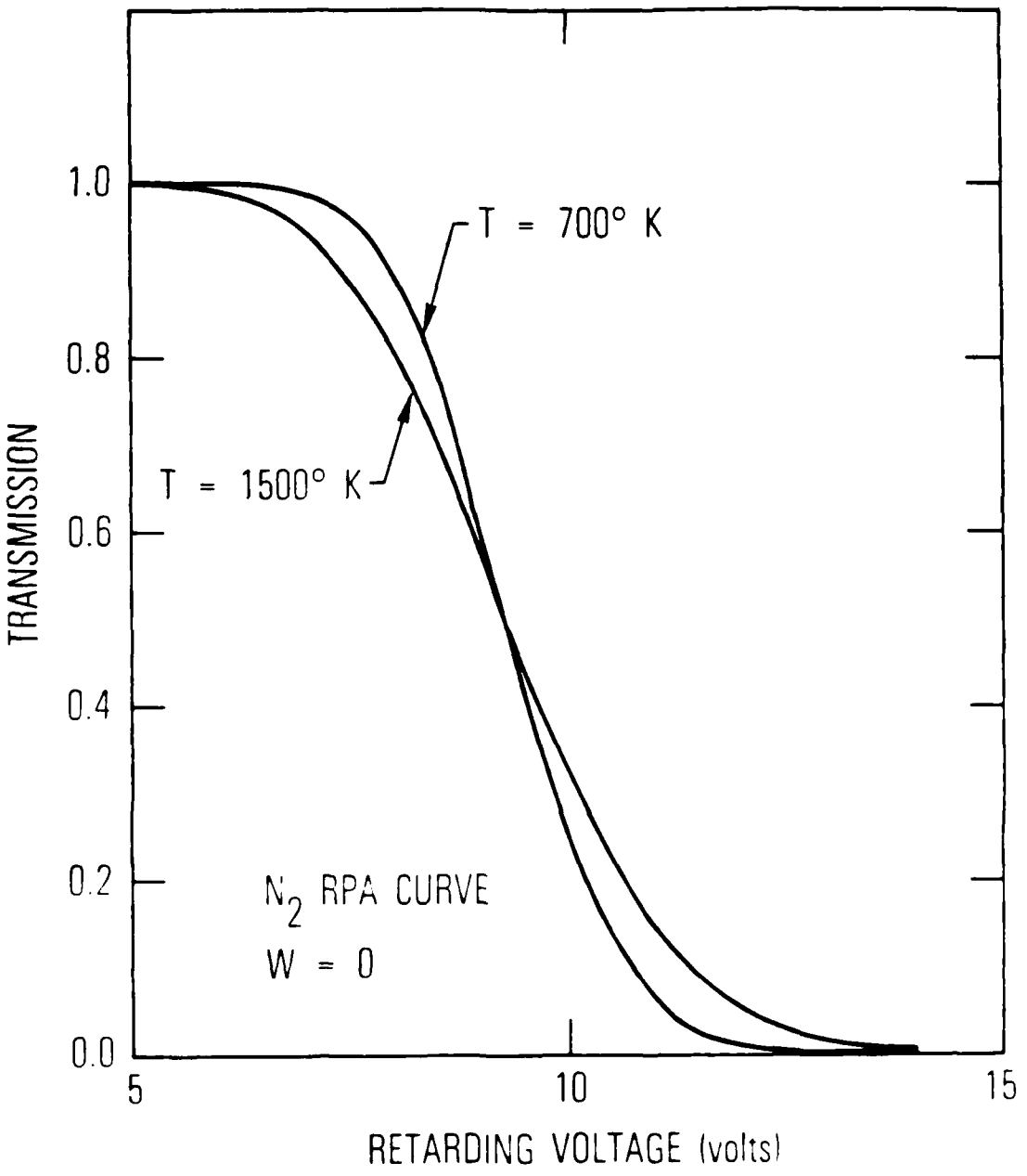

Fig. 3. Idealized Retarding Potential Transmission Curves for N_2 with Ambient Neutral Temperatures of 700 and 1500 $\mathring{K}$ and No Ram Wind Component. Temperature affects shape, not position of curve.

Previous measurement programs have shown the utility of conventional mass spectrometer measurements in the determination of He, N_2, Ar and atomic oxygen (above 220 km) composition. Additionally, with ion sources of special construction, atomic oxygen and O_2 concentrations can be obtained at all satellite altitudes.[3] The UACS was designed to exploit previous techniques, thereby providing the capability to measure complete composition in the lower thermosphere along with neutral temperature and the ram wind component. The instrument flown reflects the multiplicity of requirements and constraints of the different measurement techniques, and departs from previous experiments more in specific details, than in overall design. The remainder of this section discusses briefly some of the most important design considerations.

Angular sensitivity: At satellite velocities the streaming gas component is sharply peaked about ram with an e-folding width less than 10 degrees.[2] A sensor with high angular sensitivity would detect small departures in orientation from ram, or equivalently, cross-wind perturbations of the gas stream, as seemingly random signal variations. The quadrupole mass filter and custom-designed ion lens allow wide-angle focus, thereby minimizing this problem, while providing sufficient resolution (1-1.5 AMU) and high sensitivity.

Ion source geometry: The region where ionization occurs must view the ambient through a cone of half-angle ~ 15 degrees or more in order to fully sample the incident gas distribution. Otherwise, the RPA mode sensor output will be a function of ambient temperature. Additionally, the open geometry is necessary to illuminate the ionization chamber for the O and O_2 separation technique of Ref. 3, and has a side benefit of reducing the source background pressure. The RPA technique requires that the ionizing region, ion lens and quadrupole be in line with the gas stream.

Dynamic range: Composition measurements in the thermosphere require nearly simultaneous detection of minor species with densities of $10^6/cm^3$ or less along with major species at $10^{10}/cm^3$ or more. Also, retarding potential analysis produces inherently weak signals because it operates only on the streaming gas component. Single detector systems must compromise between detector noise limitations on the low-signal end and overload on the high-signal end. Schemes involving series detectors of different sensitivities solve the dynamic range problem but must deal with overload and possible damage to the high-sensitivity detector when high intensity peaks are selected. The UACS design places the high sensitivity detector (abbreviated in this report as SID, for spiraltron ion detector) at right angles to the quadrupole axis and employs an electrostatic deflector to steer the beam for detection of low intensity peaks.

INSTRUMENTATION

A cross-sectional view of the UACS sensor in its vacuum housing is given in Figure 4. The source vacuum cover and cutter mechanism (A) have been described previously[6] and were manufactured by the University of Minnesota Physics shops. Sealed at calibration, the sensor remains evacuated until operations in orbit are begun. At that time a cutter wheel mechanism is activated which severs the outer vacuum can. The cutter assembly and vacuum cap then deploy on a pivot arm (not shown) to an aft stored position. The source entrance collimator (B) remains to define gas flow conditions into and out of the sensor. Gas enters the ion source (C) to be ionized by a crossed electron beam from one of two redundant electron guns (D).

Ions so produced are extracted and focused by an electrostatic lens (E) into the quadrupole mass filter (F). Ions of the selected mass exit the filter into a Faraday cup (G). The cup has a small exit hole to pass a few percent of the ions. When the electrostatic deflector H is enabled, these ions are sent to the entrance cone of a Spiraltron electron multiplier (I). The cone is held at -3200 volts behind two high-transmission shield grids in the deflector assembly. Some specific details of sensor operation are found later in this section.

The sensor was designed to be entirely bakeable in order to minimize residual contamination and promote stability of electrically critical surfaces. The vacuum housing and many internal parts are of stainless steel. Electrical isolation is provided by machined ceramic stand-offs, brazed assemblies and glass feedthroughs. Vacuum flanges are gasketed with gold rings. The spiraltron electron multiplier is a bakeable model (#4219 EIL) from Galileo Electro-Optics Corporation. Before calibration the calibration

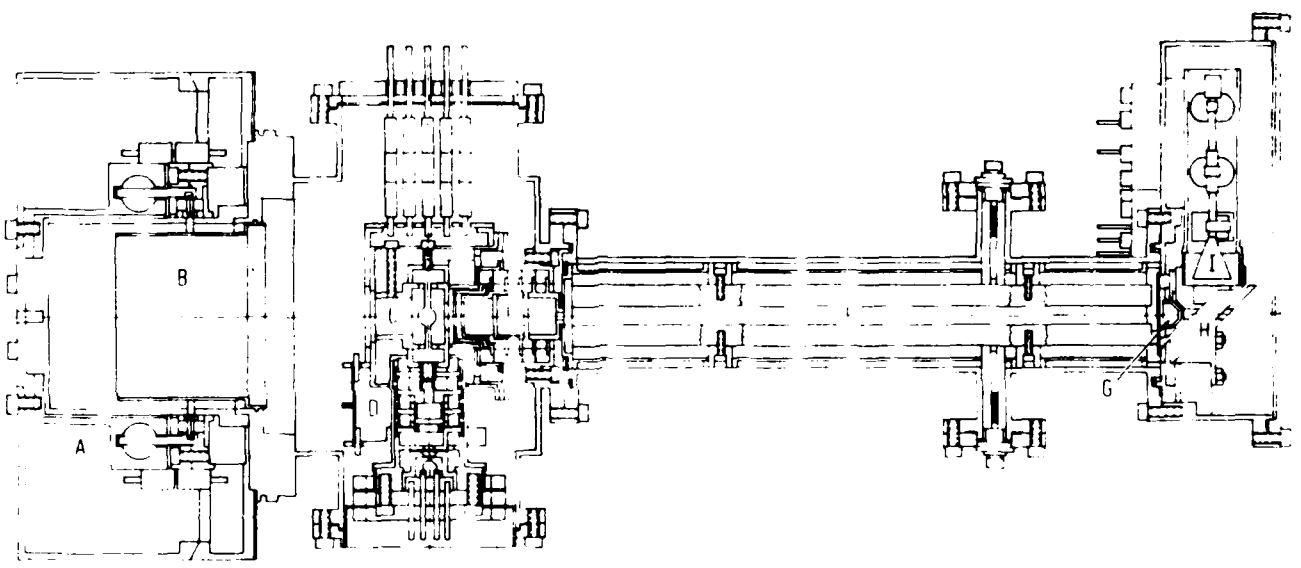

Fig. 4. UACS Sensor Including Vacuum Housing. Cap cutter mechanism (A) severs aluminum vacuum cap and retracts, exposing collimator (B) and sensor interior to the atmosphere. Crossed electron guns (D) ionize gas in chamber (C). Ions are extracted and focused by lens (E) into quadrupole mass filter (F). Ions of the selected mass are collected in electrometer cup (G) and Spiraltron multiplier (I). Voltage on deflector (H) determines whether ions reach the multiplier detector.

chamber and the mated sensor are baked at temperatures in excess of 170° C. After calibration the source vacuum cap is sealed in place without breaking vacuum. An integral Vac-Ion pump maintains high quality vacuum in the period between the end of calibration and launch. The pump is flown without a magnet and is not operated in orbit.

Figure 5 is an electrical block diagram of UACS. The instrument receives from the spacecraft 28-volt unregulated power, commands, a frequency reference, telemetry control signals, and pyrotechnic firing current. The instrument returns serial digital data at 640 b/s, two cap-cutter status bits, and four analog housekeeping voltages. The principal electronic functions include: command decode, timing and sequencing, logic and bias power supplies, filament power and regulation, quadrupole AC oscillator and DC supply, spiraltron high-voltage supply, electrometer amplifier, spiraltron pulse shaper, digital data system, and telemetry output drivers.

Instrument state is imposed by signals on the lines HVPS (high voltage power supply) on/off, Filaments on/off, Deflector Override, and Mode Control. Either of two filaments may be on, and there are five mass program modes, corresponding to a spectrum scan from 4 to 48 mass units, a scan from 4 to 48 mass units with the RPA grid set at +2 volts, energy analyze N_2, energy analyze N_2 plus sample composition at five other masses, or energy analyze in turn O, N_2, and O_2. Not all of the above options lead to useful instrument states; the most useful combinations have been recoded into a set of five-bit commands, giving 32 instrument states. Power on and off are additional commands.

The UACS instrument incorporates a number of design features which are intended to provide the high degree of stability necessary for absolute meas-

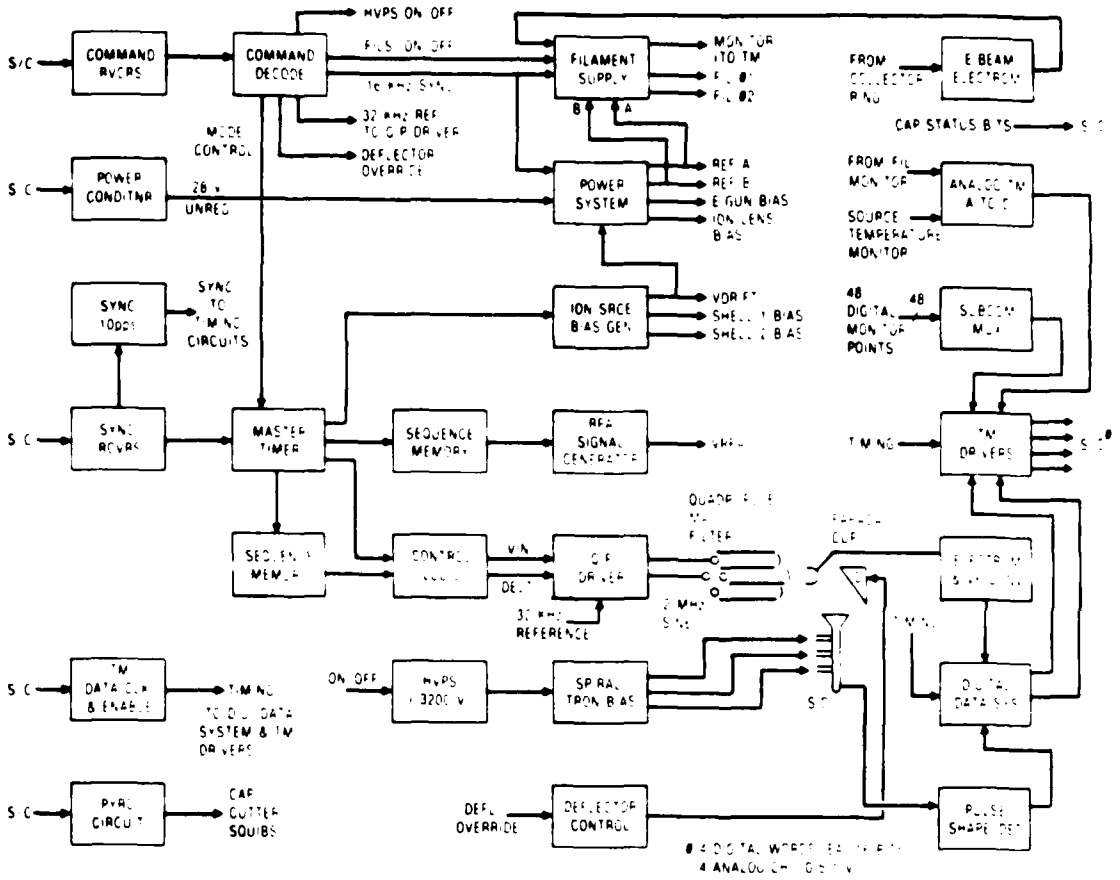

Fig. 5. UACS Electronics Block Diagram. (See text for further discussion.)

urements of composition. Constant (and known) ion source temperature facilitates the computation of ambient density via Eqn. 1. A constant and stable rate of ionization is equally important in order to derive ion source number densities from the detector signals. However, these two requirements are difficult to meet simultaneously, and past source designs have typically positioned the filaments close to the ionizing region, thereby insuring a stable electron current, but with a concomitant intense heat source that produces thermal transients at turn-on. Warmup periods of 10 to 30 minutes before data taking are therefore not uncommon for satellite-based composition experiments.

UACS uses an electrostatic lens (D, in Figure 4) to provide a parallel beam of electrons at the point of ionization, allowing the filament to be positioned 3.8 cm away. Heat generated by the filament is conducted into the vacuum flange and sensor body, and the ionization chamber is heat sunk to the ceramic spacer assembly. As a result, the ionization chamber temperature changes by only a few degrees after filament turn-on. Overall instrument temperature control is effected through surface finish of the front face and active satellite thermal control. Source temperature is monitored through a linear, calibrated temperature sensor.

With a remotely spaced filament some penalty is incurred through increased susceptibility of the electron beam to magnetic fields. The ionizing electron beam is itself regulated closed loop at 50 (± 0.1) μa using the current collected on the source collector ring (shown in Figure 6). This scheme insures that a 50 μa current crosses the chamber at the point of ionization, whereas regulation on filament emission current would not compensate for any beam transmission losses. Overall, we see on the order of a 3% change in sensor signal output for a 1-gauss external field. This level of

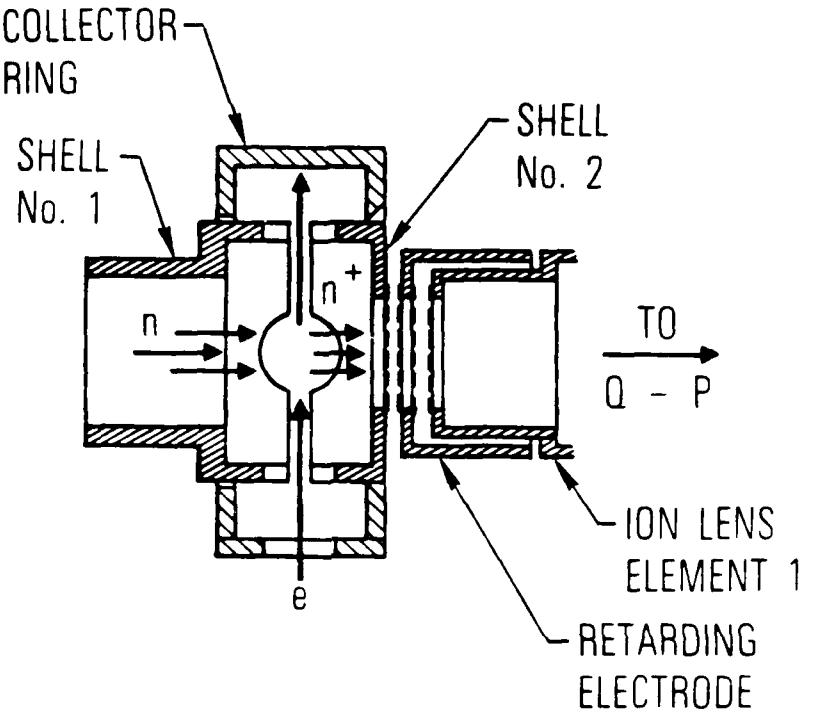

Fig. 6. Detail of Ionizing Chamber. Neutrals (n) enter at left are ionized (n+) by crossed electron beam (e) and are focused at right (complete ion lens not shown, see Fig. 4) into the quadrupole (Q-P). For normal mode Shell Nos. 1 and 2 are biased so that the +10 V potential line is along the electron-beam path and ions are accelerated toward the ion lens. For RPA mode Shell No. 1 bias equals Shell No. 2 bias, creating a drift space, and the retarding electrode voltage is swept to effect the energy analysis.

susceptibility is acceptable considering the strength of the Earth's magnetic field.

The electric field configuration of the ion lens (E, in Figure 4) was selected to provide focusing for both thermalized and streaming ions, depending on the mode of operation and to provide efficient delivery of ions into the quadrupole mass filter. The ion lens operates at large negative voltages with the last element before the quadrupole set at -200 V. Ions leaving the ionizing chamber (Figure 6) are swept rapidly into the quadrupole entrance and decelerate to an average energy of 10 ev within 0.5 cm. This is an unconventional method of injection into quadrupoles, but appears to give good transmission of ions with energies down to 3 ev. The instrumental response to streaming ions on the low energy tail is thus flatter than in conventional systems which inject at 10-15 volts. Some further details of the lens operation are given in Figure 6.

In the present design, electronics and sensor are packaged together for a total weight of 9 kg and volume of 0.021 m^3. Operating power is 8 watts, divided between electronics (2 W), filament (3 W) and quadrupole driver (3 W).

OPERATION

The 32 UACS command states provide for both low spatial resolution scan modes, which are used for diagnostics or special studies, and a variety of high spatial resolution stepping modes, the modes most expedient for routine data collection. Figure 7 is an example of on-orbit data collected in the normal (non-RPA) mass scan. The scan proceeds in 0.25 mass unit steps, ten steps per second, from mass 4 to mass 48 and then repeats. The figure shows data taken on both the electrometer (lower panel) and spiraltron (upper panel), and is an illustration of the large dynamic range obtainable with the dual detector combination. At slightly higher gas densities the deflector control circuit, which monitors the electrometer signal, would disable the SID deflector on scan steps near masses 28 (N2) and 32 (O2) so that only electrometer output would be available for the next decade increase in signal. For the combined detectors a dynamic range of a million is realized and available at each new step in the mass program. Some additional explanation of the spectrum is found in the figure caption.

Figure 8 is an example of a scan using the retarding potential gate. In this case only, the retarding gate is set +2 volts positive with respect to the drift space potential (see Fig. 6), and the drift space potential is varied with mass so that streaming ions of the selected mass exit the source with an average 10 ev total energy. It will be noted in Figure 8 that most of the peaks seen in Figure 7 have been suppressed. The remaining peaks correspond to ambient gases, O_2, N_2, and O. The mass 14 peak is attributed to ionization products of both N_2 and ambient N. Intensity in this mode is lower, corresponding to the small component of streaming gas, compared to the density of thermalized gas in the ion source.

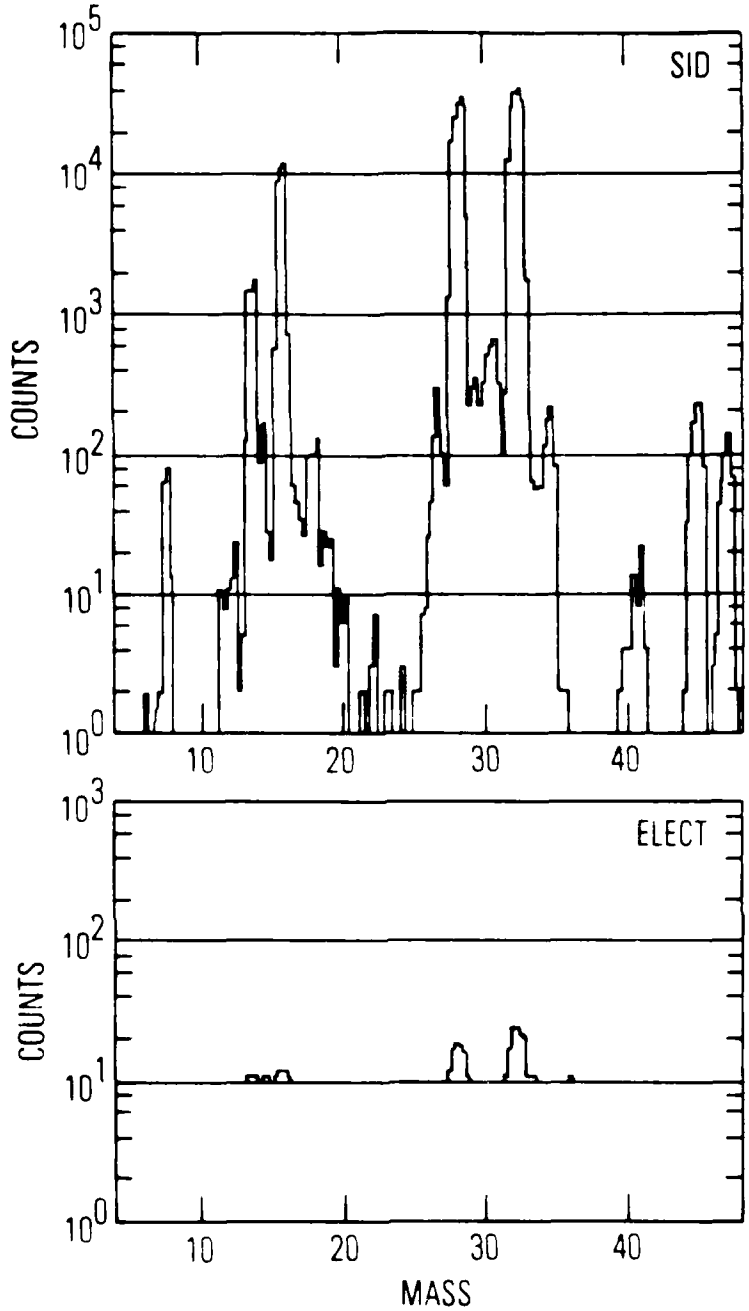

Fig. 7. Normal Mode Mass Scan on SID (Top Panel) and Electrometer (Bottom Panel) at Approximately 215 km Altitude. Peaks at masses 28, 32, 40, 44, and 46 are N_2+, O_2+, Ar+, CO_2+, NO_2+, respectively. Peaks at masses 14 and 16 result not only from singly ionized ambient N and O, but also from fractionated N_2 and O_2 and doubly ionized N_2 and O_2. The mass 32 peak results mostly from recombined atomic oxygen. Masses 30 (NO) and 46 are produced by recombination of N with O in the source. Masses 18 (H_2O) and 44 originate from source impurities.

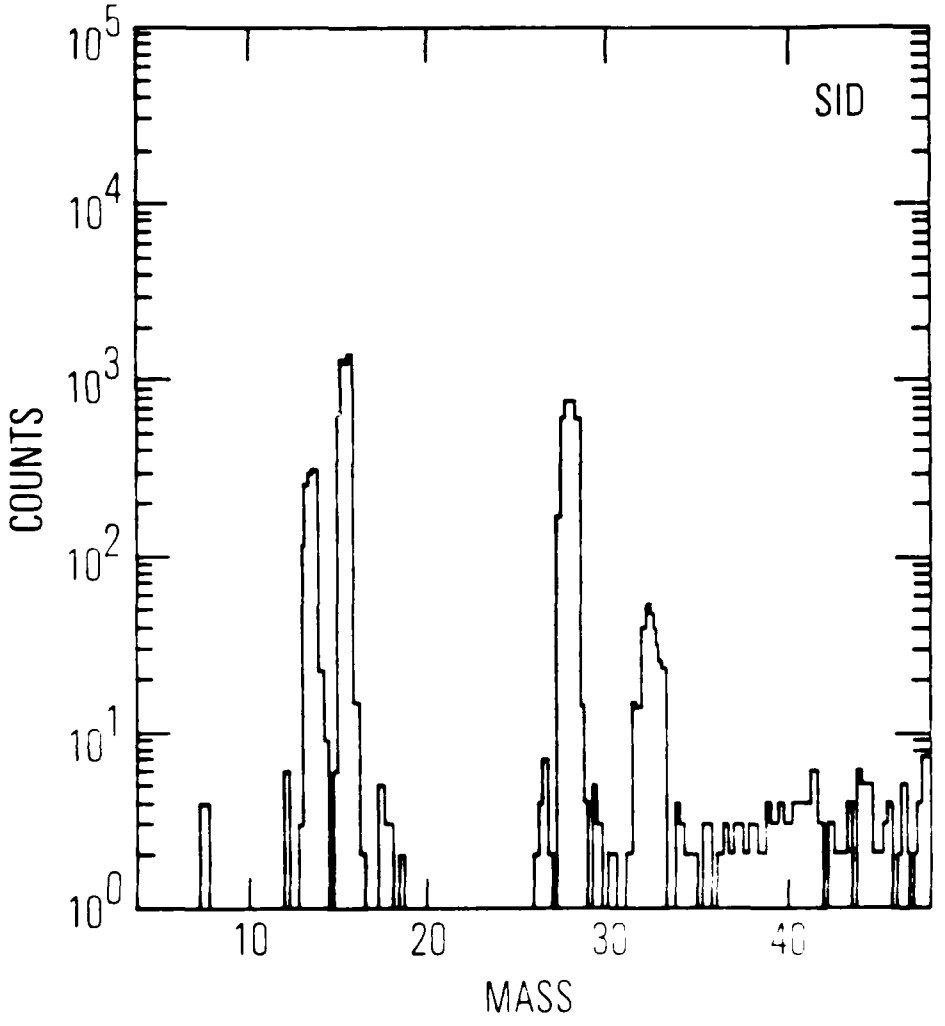

Fig. 8. Retarding (or Flythrough) Mode Scan on SID. The retarding grid potential has been set to suppress ions from the thermalized gas components. Except for a few counts background only peaks at masses 14, 16, 28, and 32 remain, corresponding respectively to ambient N, O, N_2, and O_2.

Figure 9 is an example of a typical retarding mode operation for energy analysis. Here mass is fixed at 28 (N_2) and the retarding grid is swept in 40 steps over the range from +5 to +15 volts relative to the drift space. At the start of the sweep (step A) and at its mid-point (B) the retarding grid is driven to 0 volts bias for one step to allow a normal mode determination of composition. Composition is therefore obtained at 20 km intervals along the track, concurrently with energy analysis. Ideally, the signal should drop to near zero above step 45 as the retarding potential cuts off the high energy tail of the distribution. As shown here this does not happen: In fact, a slight rise in signal is seen. During calibration a similar tail effect was noted even though the gas sample was static and no signal was obtained at lower step numbers. Thus, the tail appears to be related to reaction kinetics in the thermalized gas component, possibly in combination with focusing characteristics of the lens system.

Other retarding mode programs are available. In one, for instance, the basic cycle shown in Figure 9 is repeated at masses 16, 28 and 32 in succession, giving an energy analysis of O, N_2 and O_2. In another, the basic cycle ends with normal mode measurements at 5 selected mass numbers, allowing complete composition to be measured every 5 seconds along with the energy distribution of molecular nitrogen.

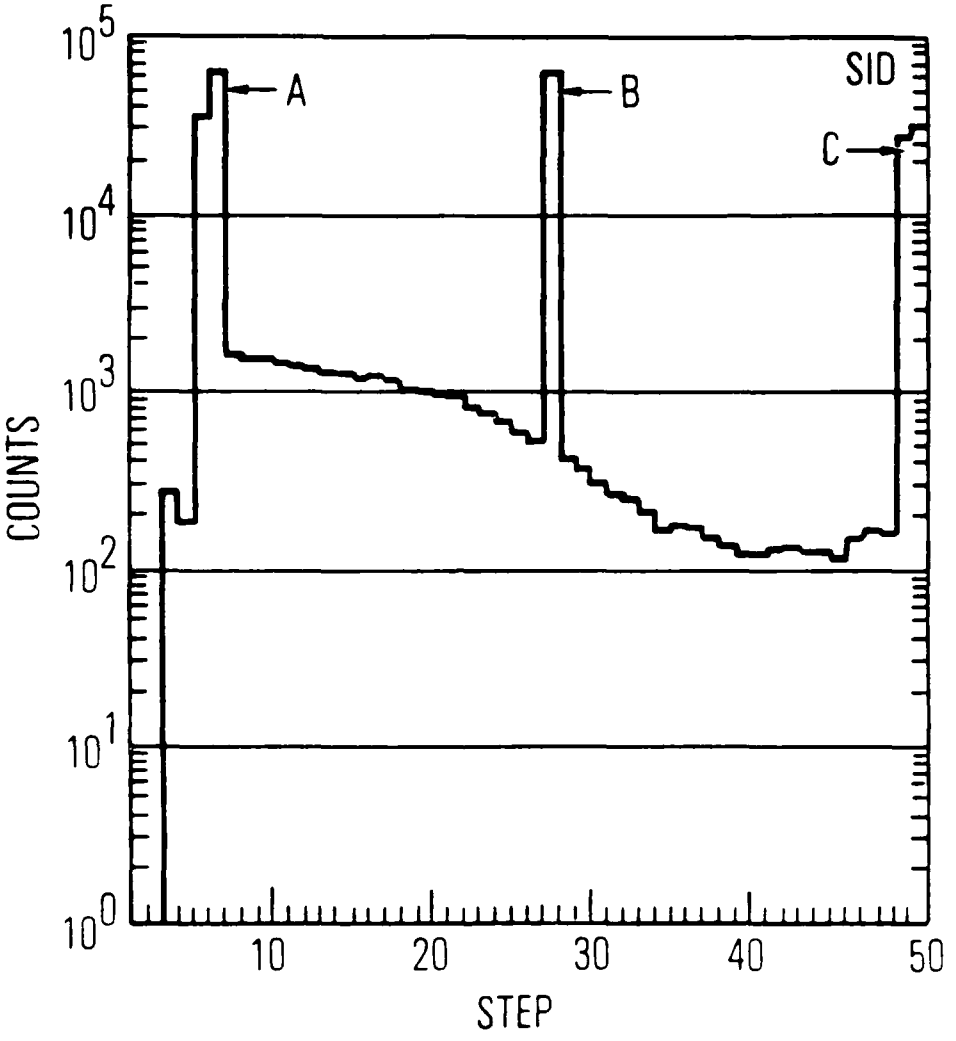

Fig. 9. Retarding Mode Energy Analysis of N_2. Steps between A and B, and between B and C comprise one RPA sweep in 4.2 sec. Steps labeled A and B are normal mode samples of the N_2 density which afford baseline composition at 20 km intervals along the track. Steps C and beyond and steps before A are not used.

CALIBRATION

Static calibration of the UACS is performed on a conventional calibration system similiar to that of Reference 8. The method involves the recording of instrument detector output as a function of the ion source pressure over the anticipated range of in-flight density. A number of sample gases are introduced into the calibration system, individually and in combination, to provide data on instrument response to most important thermospheric species. Atomic oxygen calibration is not yet practical in a static system, necessitating a cross-calibration in flight against the molecular oxygen signal. Past experience has shown that this type of calibration is a good alternative.[2,3]

PRELIMINARY FLIGHT RESULTS

Examples of flight data were shown in previous sections. The mission returned measurements sufficent to allow an evaluation of the instrument concept. It is already apparent that the basic technique of retarding potential energy analysis can be applied successfully to neutral mass analyzers. Further study should indicate ways of optimizing the design for this purpose. Besides its immediate application to aeronomic data gathering, UACS could be a starting point for a diagnostic sensor monitoring space-borne neutral-beam experiments.

SUMMARY

We have described a neutral mass analyzer package which is capable of providing both thermospheric composition data and retarding potential energy analysis of the incident neutral gas, leading to measurement of temperature and one component of the neutral wind. In addition to the energy analysis

feature, it was demonstrated that a dual detector system as described satisfies the requirement of thermospheric measurements for a large dynamic range. With further analysis we will be able to report on details of the source chemistry and on neutral thermosphere parameters during the experiment lifetime.

REFERENCES

1. Hedin, A.E., "A Revised Thermospheric Model Based on Mass Spectrometer and Incoherent Scatter Data: MSIS-83," Journal of Geophysical Research, Vol. 88, December 1983, pp.10170-10188.

2. Nier, A.O., Potter, W.E., Kayser, D.C., and Finstad, R.G., "The Measurement of Chemically Reactive Atmospheric Constituents by Mass Spectrometers Carried on High-Speed Spacecraft," Geophysical Research Letters, Vol. 1, Sept. 1974, pp. 197-200.

3. Kayser, D.C. and Potter, W.E., "A Technique for Mass Spectrometer Measurements of Atomic and Molecular Oxygen in the Lower Thermosphere," Journal of Geophysical Research, Vol. 83, March 1978, pp. 1147-1153.

4. Spencer, N.W., Niemann, H.B., and Carignan, G.R., "The Neutral- Atmosphere Temperature Instrument," Radio Science, Vol. 8, April 1973, pp. 287-296.

5. Spencer, N.W., Wharton, L.E., Nieman, H.B., Hedin, A.E., Carignan, G.R. and Maurer, J.C., "The Dynamics Explorer Wind and Temperature Spectrometer," Space Science Instrumentation, Vol. 5, 1981, pp. 417-427.

6. Nier, A.O., Potter, W.E., Hickman, D.R., and Mauersberger, K., "The Open-Source Neutral-Mass Spectrometer on Atmosphere Explorer- C, -D, and -E," Radio Science, Vol. 8, April 1973, pp. 271-276.

7. Peltz, D.T., Reber, C.A., Hedin, A.E., and Carignan, G.R., "A Neutral-Atmosphere Composition Experiment for the Atmosphere Explorer-C, -D, and -E," Radio Science, Vol. 8, April 1973, pp. 277-285.

8. Hedin, A.E., Avery, C.P., and Tschetter, C.D., "An Analysis of Spin Modulation Effects on Data Obtained with a Rocket-Borne Mass Spectrometer," Journal of Geophysical Research, Vol. 69, November 1964, pp. 4637-4648.

9. Kayser, D.C., and Potter, W.E., "Molecular Oxygen Measurements at 200 Km from AE-D near Winter Solstice," Geophysical Research Letters, Vol. 3, August 1976, pp. 455-458.

10. Knutson, J.R., Kayser, D.C., and Potter, W.E., "Mass Spectrometric Measurement of Thermospheric Wind," Journal of Geophysical Research, Vol. 82, November 1977, pp. 5253-5256.

11. Hoffman, R.A. and Schmerling, E.R., "Dynamics Explorer Program: An Overview," Space Science Instrumentation, Vol. 5, 1981, pp. 345-348.

LABORATORY OPERATIONS

The Aerospace Corporation functions as an "architect-engineer" for national security projects, specializing in advanced military space systems. Providing research support, the corporation's Laboratory Operations conducts experimental and theoretical investigations that focus on the application of scientific and technical advances to such systems. Vital to the success of these investigations is the technical staff's wide-ranging expertise and its ability to stay current with new developments. This expertise is enhanced by a research program aimed at dealing with the many problems associated with rapidly evolving space systems. Contributing their capabilities to the research effort are these individual laboratories:

Aerophysics Laboratory: Launch vehicle and reentry fluid mechanics, heat transfer and flight dynamics; chemical and electric propulsion, propellant chemistry, chemical dynamics, environmental chemistry, trace detection; spacecraft structural mechanics, contamination, thermal and structural control; high temperature thermomechanics, gas kinetics and radiation; cw and pulsed chemical and excimer laser development including chemical kinetics, spectroscopy, optical resonators, beam control, atmospheric propagation, laser effects and countermeasures.

Chemistry and Physics Laboratory: Atmospheric chemical reactions, atmospheric optics, light scattering, state-specific chemical reactions and radiative signatures of missile plumes, sensor out-of-field-of-view rejection, applied laser spectroscopy, laser chemistry, laser optoelectronics, solar cell physics, battery electrochemistry, space vacuum and radiation effects on materials, lubrication and surface phenomena, thermionic emission, photosensitive materials and infrared detectors, atomic frequency standards, and environmental chemistry.

Computer Science Laboratory: Program verification, program translation, performance-sensitive system design, distributed architectures for spaceborne computers, fault-tolerant computer systems, artificial intelligence, microelectronics applications, communication protocols, and computer security.

Electronics Research Laboratory: Microelectronics, solid-state device physics, compound semiconductors, radiation hardening; electro-optics, quantum electronics, solid-state lasers, optical propagation and communications; microwave semiconductor devices, microwave/millimeter wave measurements, diagnostics and radiometry, microwave/millimeter wave thermonic devices; atomic time and frequency standards; antennas, RF systems, electromagnetic propagation phenomena, space communication systems.

Materials Sciences Laboratory: Development of new materials: metals, alloys, ceramics, polymers and their composites, and new forms of carbon; nondestructive evaluation, component failure analysis and reliability; fracture mechanics and stress corrosion; analysis and evaluation of materials at cryogenic and elevated temperatures as well as in space and enemy-induced environments.

Space Sciences Laboratory: Magnetospheric, auroral and cosmic ray physics, wave-particle interactions, magnetospheric plasma waves; atmospheric and ionospheric physics, density and composition of the upper atmosphere, remote sensing using atmospheric radiation; solar physics, infrared astronomy, infrared signature analysis; effects of solar activity, magnetic storms and nuclear explosions on the earth's atmosphere, ionosphere and magnetosphere; effects of electromagnetic and particulate radiations on space systems; space instrumentation.

END

2-87

DTIC